Int. J. Solids Structures Vol. 23, No. 4, pp. 485–503, 1987
Printed in Great Britain.

0020-7683/87 $3.00+.00
Pergamon Journals Ltd.

TORSION OF A MICROPOLAR ELASTIC PRISM OF SQUARE CROSS-SECTION

H. C. PARK
Departments of Mechanical Engineering, University of Iowa, Iowa City, IA 52242, U.S.A.
NOW AT POHANG - KOREA
POSTECH and

R. S. LAKES
Departments of Biomedical Engineering and Mechanical Engineering, University of [redacted], [redacted], U.S.A.
WISCONSIN, Madison WI

(*Received* 22 *October* 1985; *in revised form* 15 *April* 1986)

Abstract—An analytical solution is presented for the problem of torsion of a prismatical bar of square cross-section of a micropolar (Cosserat) elastic solid. Warp of the cross-sections is found to differ from the warp in a classically elastic solid. Contrary to the classical case, a non-zero shear strain is predicted to occur at the edge of the bar. Novel experimental modalities are suggested on the basis of this analytical solution.

1. INTRODUCTION

This study is motivated in part by the desire to develop improved experimental modalities for the study of Cosserat elastic media. Previous experiments intended to obtain evidence of Cosserat elastic behavior, have utilized the size effects predicted to occur in inhomogeneous deformation (e.g. torsion and bending) of Cosserat solids. Such experiments have disclosed classical behavior[1–4] or Cosserat elastic behavior[4–7] depending on the material. In its recent forms, the method of size effects is capable of determining all six elastic constants of an isotropic Cosserat solid[7]. Nevertheless, the method is tedious since specimens must be progressively cut to smaller sizes, or an ensemble of specimens of identical properties and different size must be obtained. In addition, the range of specimen size must include sizes not greatly in excess of the size of the microstructure. If the structural element size is small, the preparation of these specimens presents an additional challenge to the experimentalist.

In this article, the problem of torsion of a prism of square cross-section, of a linear isotropic Cosserat solid, is solved analytically. Experimental modalities for Cosserat solids are developed on the basis of this solution.

2. BASIC EQUATIONS

Consider a linear micropolar (i.e. Cosserat) elastic medium which is macroscopically homogeneous and isotropic. Assume that body forces and body couples vanish. The basic equations in the static theory of homogeneous and isotropic micropolar elastic solids are as follows[8]. In this section, the Einstein summation convention for summation over repeated indices is used. A comma followed by a subscript denotes partial differentiation with respect to the corresponding Cartesian coordinate.

The equilibrium equations are

$$t_{ji,i} = 0 \tag{1}$$

$$m_{ji,j} + e_{ikl}t_{kl} = 0 \tag{2}$$

in which t_{ji} is the Cauchy stress, m_{ji} is the couple stress, and e_{ikl} is the permutation symbol.

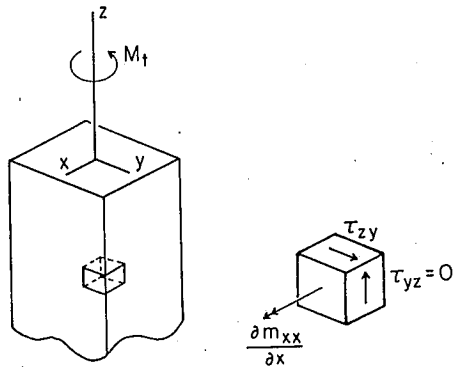

Fig. 1. Differential element at the corner of a cross-section of a twisted bar.

The constitutive equations are

$$t_{ij} = \lambda\varepsilon_{kk}\delta_{ij} + (\mu + \kappa)\varepsilon_{ij} + \mu\varepsilon_{ji} \tag{3}$$

$$m_{ij} = \alpha\phi_{k,k}\delta_{ij} + \beta\phi_{i,j} + \gamma\phi_{j,i} \tag{4}$$

in which ε_{ij} is the micropolar strain, defined below, ϕ_i is the microrotation vector, and λ, μ, κ, α, β and γ are the six independent elastic constants of an isotropic micropolar (Cosserat) solid.

The strain–displacement relations are

$$\varepsilon_{ij} = u_{j,i} + e_{jik}\phi_k = e_{ij} + e_{ijm}(r_m - \phi_m) \tag{5}$$

in which u_j is the displacement vector, $e_{ij} = (u_{i,j} + u_{j,i})/2$ is the conventional strain, and r_m is the macrorotation vector $r_m = e_{mln}u_{n,l}/2$. The surface tractions and surface couples acting on a bounding surface S of a body are given by

$$t_i = t_{ji}n_j$$

$$m_i = m_{ji}n_j$$

where n_j is the unit vector of the outward normal to S at the point.

3. CORNER DIFFERENTIAL ELEMENT

To develop insight into the structure of the solution to the torsion problem, consider a differential element at the corner of a cross-section, as shown in Fig. 1. In a classically elastic solid, one may argue on the basis of the stress boundary conditions on the lateral surface, and the symmetry of the stress tensor, that the shear stress vanishes at the corner[9]. In a Cosserat solid, the stress tensor can be asymmetric, as seen in the expanded form of equilibrium eqn (2)

$$\frac{\partial m_{xx}}{\partial x} + \frac{\partial m_{yx}}{\partial y} + \frac{\partial m_{zx}}{\partial z} + t_{yz} - t_{zy} = 0. \tag{6}$$

For the corner element

$$t_{yz} = 0, \quad m_{yx} = 0, \quad m_{yz} = 0, \quad \text{and} \quad m_{yy} = 0 \quad \text{on} \quad y = \pm\frac{a}{2}$$

$$t_{xz} = 0, \quad m_{xy} = 0, \quad m_{xz} = 0, \quad \text{and} \quad m_{xx} = 0 \quad \text{on} \quad x = \pm\frac{a}{2}$$

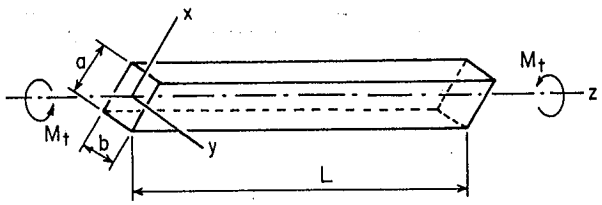

Fig. 2. Torsion of a prism of rectangular cross-section.

But $\partial m_{xx}/\partial x$, $\partial m_{yx}/\partial y$ and $\partial m_{zx}/\partial z$ are not equal to zero in general, so in eqn (6) $t_{zy} \neq 0$. The corner element, therefore, can experience shear stress, in contrast to the classical case.

From the constitutive eqns (3), $t_{yz} = (2\mu + \kappa)e_{zy} + \kappa(r_x - \phi_x)$ in which e_{zy} and r_x are classical shear strain and rotation (macrorotation), respectively. For the corner element

$$t_{yz} = 0 = (2\mu + \kappa)e_{zy} + \kappa(r_x - \phi_x).$$

Since the macrorotation and microrotation are different in general

$$e_{zy} = -\frac{\kappa}{2\mu + \kappa}(r_x - \phi_x). \tag{7}$$

Therefore, the corner element experiences shear strain, unlike the classical case.

4. TORSION OF PRISM OF RECTANGULAR CROSS-SECTION

Consider a prismatic bar of rectangular cross-section subject to equal and opposite twisting moments at the ends, as in Fig. 2. Let one side of the cross-section, of length a, be parallel to the x-axis and that of length b be parallel to the y-axis. It will be supposed that $b \geqslant a$ and that the z-axis passes through the center of the cross-section.

4.1. *Governing equations*

Boundary value problems involving rectangular cross-sections are most conveniently treated in Cartesian coordinates, (x, y, z). The governing equations for a micropolar solid are therefore presented in expanded form, in Cartesian coordinates.

Equilibrium

$$\frac{\mathrm{d}}{\mathrm{d}x}\begin{bmatrix} t_{xx} \\ t_{xy} \\ t_{xz} \end{bmatrix} + \frac{\mathrm{d}}{\mathrm{d}y}\begin{bmatrix} t_{yx} \\ t_{yy} \\ t_{yz} \end{bmatrix} + \frac{\mathrm{d}}{\mathrm{d}z}\begin{bmatrix} t_{zx} \\ t_{zy} \\ t_{zz} \end{bmatrix} = 0 \tag{8a}$$

$$\frac{\mathrm{d}}{\mathrm{d}x}\begin{bmatrix} m_{xx} \\ m_{xy} \\ m_{xz} \end{bmatrix} + \frac{\mathrm{d}}{\mathrm{d}y}\begin{bmatrix} m_{yx} \\ m_{yy} \\ m_{yz} \end{bmatrix} + \frac{\mathrm{d}}{\mathrm{d}z}\begin{bmatrix} m_{zx} \\ m_{zy} \\ m_{zz} \end{bmatrix} + \begin{bmatrix} t_{yz} - t_{zy} \\ t_{zx} - t_{xz} \\ t_{xy} - t_{yx} \end{bmatrix} = 0. \tag{8b}$$

Constitutive

$$\begin{bmatrix} t_{xx} \\ t_{yy} \\ t_{zz} \end{bmatrix} = \lambda(\varepsilon_{xx} + \varepsilon_{yy} + \varepsilon_{zz}) + (2\mu + \kappa)\begin{bmatrix} \varepsilon_{xx} \\ \varepsilon_{yy} \\ \varepsilon_{zz} \end{bmatrix} \tag{9a}$$

$$\begin{bmatrix} t_{xy} \\ t_{xz} \\ t_{yx} \\ t_{yz} \\ t_{zx} \\ t_{zy} \end{bmatrix} = (\mu + \kappa) \begin{bmatrix} \varepsilon_{xy} \\ \varepsilon_{xz} \\ \varepsilon_{yx} \\ \varepsilon_{yz} \\ \varepsilon_{zx} \\ \varepsilon_{zy} \end{bmatrix} + \mu \begin{bmatrix} \varepsilon_{yx} \\ \varepsilon_{zx} \\ \varepsilon_{xy} \\ \varepsilon_{zy} \\ \varepsilon_{xz} \\ \varepsilon_{yz} \end{bmatrix} \tag{9b}$$

$$\begin{bmatrix} m_{xx} \\ m_{yy} \\ m_{zz} \end{bmatrix} = \alpha \left(\frac{\partial \phi_x}{\partial x} + \frac{\partial \phi_y}{\partial y} + \frac{\partial \phi_z}{\partial z} \right) + (\beta + \gamma) \begin{bmatrix} \partial \phi_x / \partial x \\ \partial \phi_y / \partial y \\ \partial \phi_z / \partial z \end{bmatrix} \tag{9c}$$

$$\begin{bmatrix} m_{xy} \\ m_{xz} \\ m_{yx} \\ m_{yz} \\ m_{zx} \\ m_{zy} \end{bmatrix} = \beta \begin{bmatrix} \partial \phi_x / \partial y \\ \partial \phi_x / \partial z \\ \partial \phi_y / \partial x \\ \partial \phi_y / \partial z \\ \partial \phi_z / \partial x \\ \partial \phi_z / \partial y \end{bmatrix} + \gamma \begin{bmatrix} \partial \phi_y / \partial x \\ \partial \phi_z / \partial x \\ \partial \phi_x / \partial y \\ \partial \phi_z / \partial y \\ \partial \phi_x / \partial z \\ \partial \phi_y / \partial z \end{bmatrix}. \tag{9d}$$

Strain–displacement

$$\begin{bmatrix} \varepsilon_{xx} \\ \varepsilon_{yy} \\ \varepsilon_{zz} \end{bmatrix} = \begin{bmatrix} \partial u_x / \partial x \\ \partial u_y / \partial y \\ \partial u_z / \partial z \end{bmatrix} \tag{10a}$$

$$\begin{bmatrix} \varepsilon_{xy} \\ \varepsilon_{xz} \\ \varepsilon_{yx} \\ \varepsilon_{yz} \\ \varepsilon_{zx} \\ \varepsilon_{zy} \end{bmatrix} = \begin{bmatrix} \partial u_y / \partial x \\ \partial u_z / \partial x \\ \partial u_x / \partial y \\ \partial u_z / \partial y \\ \partial u_x / \partial z \\ \partial u_y / \partial z \end{bmatrix} + \begin{bmatrix} -\phi_z \\ \phi_y \\ \phi_z \\ -\phi_x \\ -\phi_y \\ \phi_x \end{bmatrix}. \tag{10b}$$

Equilibrium equations in terms of displacements. Substitution of constitutive equations into equilibrium equations yields equilibrium equations in terms of displacement. They are

$$(\lambda + 2\mu + \kappa)u_{x,xx} + (\mu + \kappa)(u_{x,yy} + u_{x,zz}) + (\lambda + \mu)(u_{y,xy} + u_{z,xz}) + \kappa(\phi_{z,y} - \phi_{y,z}) = 0 \tag{11a}$$

$$(\lambda + 2\mu + \kappa)u_{y,yy} + (\mu + \kappa)(u_{y,xx} + u_{y,zz}) + (\lambda + \mu)(u_{x,xy} + u_{z,yz}) + \kappa(\phi_{x,z} - \phi_{z,x}) = 0 \tag{11b}$$

$$(\lambda + 2\mu + \kappa)u_{z,zz} + (\mu + \kappa)(u_{z,xx} + u_{z,yy}) + (\lambda + \mu)(u_{x,xz} + u_{y,zy}) + \kappa(\phi_{y,x} - \phi_{x,y}) = 0 \tag{11c}$$

$$(\alpha + \beta + \gamma)\phi_{x,xx} + (\alpha + \beta)(\phi_{y,xy} + \phi_{z,xz}) + \gamma(\phi_{x,yy} + \phi_{x,zz}) + \kappa[(u_{z,y} - u_{y,z}) - 2\phi_x] = 0 \tag{11d}$$

$$(\alpha + \beta + \gamma)\phi_{y,yy} + (\alpha + \beta)(\phi_{x,xy} + \phi_{z,yz}) + \gamma(\phi_{y,xx} + \phi_{y,zz}) + \kappa[(u_{x,z} - u_{z,x}) - 2\phi_y] = 0 \tag{11e}$$

$$(\alpha + \beta + \gamma)\phi_{z,zz} + (\alpha + \beta)(\phi_{x,xz} + \phi_{y,yz}) + \gamma(\phi_{z,xx} + \phi_{z,yy}) + \kappa[(u_{y,x} - u_{x,y}) - 2\phi_z] = 0. \tag{11f}$$

4.2. *Compatibility conditions*

$$\frac{\partial \varepsilon_{xx}}{\partial y} - \frac{\partial \varepsilon_{yx}}{\partial x} + \frac{\partial \phi_z}{\partial x} = 0 \tag{12a}$$

$$\frac{\partial \varepsilon_{xy}}{\partial y} - \frac{\partial \varepsilon_{yy}}{\partial x} + \frac{\partial \phi_z}{\partial y} = 0 \tag{12b}$$

$$\frac{\partial \varepsilon_{xz}}{\partial z} - \frac{\partial \varepsilon_{yz}}{\partial x} - \frac{\partial \phi_y}{\partial y} - \frac{\partial \phi_x}{\partial x} = 0 \tag{12c}$$

$$\frac{\partial \varepsilon_{xx}}{\partial z} - \frac{\partial \varepsilon_{zx}}{\partial x} - \frac{\partial \phi_y}{\partial x} = 0 \tag{12d}$$

$$\frac{\partial \varepsilon_{xy}}{\partial z} - \frac{\partial \varepsilon_{zy}}{\partial x} + \frac{\partial \phi_z}{\partial z} + \frac{\partial \phi_x}{\partial x} = 0 \tag{12e}$$

$$\frac{\partial \varepsilon_{xz}}{\partial z} - \frac{\partial \varepsilon_{zz}}{\partial x} - \frac{\partial \phi_y}{\partial z} = 0 \tag{12f}$$

$$\frac{\partial \varepsilon_{yx}}{\partial z} - \frac{\partial \varepsilon_{zx}}{\partial y} - \frac{\partial \phi_z}{\partial z} - \frac{\partial \phi_y}{\partial y} = 0 \tag{12g}$$

$$\frac{\partial \varepsilon_{yy}}{\partial \varepsilon_z} - \frac{\partial \varepsilon_{zy}}{\partial y} + \frac{\partial \phi_x}{\partial y} = 0 \tag{12h}$$

$$\frac{\partial \varepsilon_{yz}}{\partial z} - \frac{\partial \varepsilon_{zz}}{\partial y} + \frac{\partial \phi_x}{\partial z} = 0. \tag{12i}$$

4.3. *Stress boundary conditions*

On the boundary surface S of a body

$$\begin{bmatrix} t_{(n)x} \\ t_{(n)y} \\ t_{(n)z} \end{bmatrix} = n_x \begin{bmatrix} t_{xx} \\ t_{xy} \\ t_{xz} \end{bmatrix} + n_y \begin{bmatrix} t_{yx} \\ t_{yy} \\ t_{yz} \end{bmatrix} + n_z \begin{bmatrix} t_{zx} \\ t_{zy} \\ t_{zz} \end{bmatrix} \tag{13a}$$

$$\begin{bmatrix} m_{(n)x} \\ m_{(n)y} \\ m_{(n)z} \end{bmatrix} = n_x \begin{bmatrix} m_{xx} \\ m_{xy} \\ m_{xz} \end{bmatrix} + n_y \begin{bmatrix} m_{yx} \\ m_{yy} \\ m_{yz} \end{bmatrix} + n_z \begin{bmatrix} m_{zx} \\ m_{zy} \\ m_{zz} \end{bmatrix}. \tag{13b}$$

5. SOLUTION

5.1. *Determination of field of displacement and microrotation*

Iesan[10, 11] has proven the existence of solution for the general torsion problem and the uniqueness theorem[8] ensures the uniqueness of the solution once it is found.

A semi-inverse method will be used to solve the problem. Since the cross-sections are noncircular, they will experience warp u_z when the bar is twisted. The solution is constructed by superposition from the following fields of displacement and microrotation, which shall be denoted by {I} and {II}.

Field {I}:

$$u_x = -\theta yz \tag{14a}$$

$$u_y = \theta xz \tag{14b}$$

$$u_z = \theta xy - \theta \sum_{n=0}^{\infty} B_n \sinh(k_n y) \sin(k_n x) \tag{14c}$$

$$\phi_x = -\theta \sum_{n=0}^{\infty} \tfrac{1}{2} B_n k_n \cosh(k_n y) \sin(k_n x) \tag{14d}$$

$$\phi_y = -\theta y + \theta \sum_{n=0}^{\infty} \tfrac{1}{2} B_n k_n \sinh(k_n y) \cos(k_n x) \tag{14e}$$

$$\phi_z = \theta z. \tag{14f}$$

Field $C\{\mathrm{II}\}$:

$$u_x = -\theta Cyz \tag{15a}$$

$$u_y = \theta Cxz \tag{15b}$$

$$u_z = \theta Cxy - \theta C \sum_{n=0}^{\infty} A_n \sinh(p_n y) \sin(k_n x) \tag{15c}$$

$$\phi_x = -\theta C \sum_{n=0}^{\infty} D_n \sinh(p_n y) \sin(k_n x) \tag{15d}$$

$$\phi_y = -\theta Cy - \theta C \sum_{n=0}^{\infty} F_n \sinh(p_n y) \cos(k_n x) \tag{15e}$$

$$\phi_z = \theta Cz. \tag{15f}$$

Here θ is a twist angle per unit length, $k_n = (2n+1)\pi/a$, $B_n = 8(-1)^n/ak_n^3 \cosh(k_n b/2)$, and A_n, D_n, P_n and C are to be determined. Field $\{\mathrm{I}\}$ may be recognized as identical to the solution in classical elasticity[9], with the microrotations ϕ set equal to the classical macrorotations.

Consider now the superposition $\{\mathrm{I}\} + C\{\mathrm{II}\}$. Substituting this field into the equilibrium equations, one obtains

$$\sum_{n=0}^{\infty} \{(\mu+\kappa)[A_n k_n^2 - A_n p_n^2] - \kappa[F_n k_n - D_n p_n]\} \sinh(p_n y) \sin(k_n x) = 0 \tag{16a}$$

$$\sum_{n=0}^{\infty} \{(\alpha+\beta+\gamma) D_n k_n^2 - (\alpha+\beta) F_n k_n p_n - \gamma D_n p_n^2 - \kappa A_n p_n + 2D_n\} \cosh(p_n y) \sin(k_n x) = 0 \tag{16b}$$

$$\sum_{n=0}^{\infty} \{(\alpha+\beta+\gamma) F_n p_n^2 - (\alpha+\beta) D_n k_n p_n - \gamma F_n k_n^2 + \kappa A_n k_n - 2F_n\} \sinh(p_n y) \cos(k_n x) = 0 \tag{16c}$$

and eqns (11a), (11b) and (11f) are identically satisfied.

From eqn (16a), we obtain

$$(\mu+\kappa)[A_n k_n^2 + A_n p_n^2] + \kappa[D_n p_n - F_n k_n] = 0 \tag{17a}$$

or

$$k_n^2 - p_n^2 = 2N^2 \frac{F_n k_n - D_n p_n}{A_n} \tag{17b}$$

where N is the coupling number[12]

$$N^2 = \frac{\kappa}{2(\mu + \kappa)}.$$

Upon rearranging and combining eqns (16b) and (16c) we obtain

$$\kappa[A_n(p_n^2 - k_n^2) - 2(D_n p_n - F_n k_n)] = \gamma(D_n p_n - F_n k_n)(k_n^2 - p_n^2).$$

Upon using eqn (17b) we obtain

$$p_n^2 = k_n^2 + \left(\frac{N}{l_b}\right)^2 \tag{18}$$

where l_b is a characteristic length, originally encountered in the context of bending problems[3]

$$l_b^2 = \frac{\gamma}{2(2\mu + \kappa)}.$$

For boundary conditions we prescribe first that the lateral surfaces, $x = \pm a/2$ and $y = \pm b/2$, be free of all tractions and couples

$$t_{(n)x} = t_{(n)y} = t_{(n)z} = m_{(n)x} = m_{(n)y} = m_{(n)z} = 0.$$

We apply eqns (13a) and (13b) and obtain

$$t_{xx} = t_{xz} = 0 \qquad \text{on } x = \pm \frac{a}{2} \tag{19a}$$

$$t_{yy} = t_{yz} = 0 \qquad \text{on } y = \pm \frac{b}{2} \tag{19b}$$

$$m_{xx} = m_{xy} = 0 \qquad \text{on } x = \pm \frac{a}{2} \tag{19c}$$

$$m_{yy} = m_{yx} = 0 \qquad \text{on } y = \pm \frac{b}{2}. \tag{19d}$$

It is prescribed on the end surfaces $z = 0$ and L that the distribution of stress and couple stress be equipollent to a twisting moment M_t and zero net force

$$\int_A t_{(n)z}\, \mathrm{d}A = 0 \tag{20a}$$

$$\int_A (x t_{zy} - y t_{zx} + m_{zz})\, \mathrm{d}A = M_t. \tag{20b}$$

From eqns (19a)–(19d) and the constitutive equations we obtain

$$t_{xz}|_{x=a/2} = \sum_{n=0}^{\infty} \{\kappa F_n - (\mu + \kappa)A_n k_n\} \cos\left(k_n \frac{a}{2}\right) \sinh(p_n y).$$

Since

$$\cos\left(k_n \frac{a}{2}\right) = 0, \qquad t_{xz}|_{x=a/2} = 0$$

is always satisfied.

$$t_{yz}|_{y=b/2} = (2\mu + \kappa)x - \sum_{n=0}^{\infty} \{(\mu + \kappa)A_n p_n - \kappa D_n\} \cosh\left(p_n \frac{b}{2}\right) \sin(k_n x) = 0. \tag{21}$$

Upon expanding the first term of eqn (21) into a Fourier sine series in $[-a, a]$

$$\sum_{n=0}^{\infty} \left\{(2\mu + \kappa)\frac{4(-1)^n}{ak_n^2} - [(\mu + \kappa)A_n p_n - \kappa D_n] \cosh\left(p_n \frac{b}{2}\right)\right\} \sin(k_n x) = 0.$$

Since this has to hold for all x

$$(2\mu + \kappa)\frac{4(-1)^n}{ak_n^2} - [(\mu + \kappa)A_n p_n - \kappa D_n] \cosh\left(p_n \frac{b}{2}\right) = 0$$

thus

$$A_n = \frac{\kappa}{\mu + \kappa}\frac{D_n}{p_n} + \frac{2\mu + \kappa}{\mu + \kappa}\frac{4(-1)^n}{ak^2 p_n \cosh\left(p_n \frac{b}{2}\right)}$$

or

$$A_n = 2N^2 \frac{D_n}{p_n} + (1 - N^2)\frac{8(-1)^n}{ak_n^2 p_n \cosh\left(p_n \frac{b}{2}\right)}. \tag{22}$$

Now

$$m_{xx}|_{x=a/2} = \sum_{n=0}^{\infty} \{\alpha F_n p_n - (\alpha + \beta + \gamma)D_n k_n\} \cos\left(k_n \frac{a}{2}\right) \sinh(p_n y)$$

since

$$\cos\left(k_n \frac{a}{2}\right) = 0, \qquad m_{xx}|_{x=a/2} = 0$$

is always satisfied

$$m_{yy}|_{y=b/2} = \sum_{n=0} \{(\alpha + \beta + \gamma)F_n p_n - \alpha D_n k_n\} \cosh\left(p_n \frac{b}{2}\right) \cos(k_n x) - (\beta + \gamma) = 0. \tag{23}$$

Upon transforming the last term of eqn (23) to a Fourier cosine series in $[-b, b]$

$$\sum_{n=0}^{\infty} \{(\alpha+\beta+\gamma)F_n p_n - \alpha D_n k_n\} \cosh\left(p_n \frac{b}{2}\right) - (\beta+\gamma)\frac{4(-1)^n}{ak_n}\Bigg\} \cos(k_n x) = 0.$$

Since this has to hold for all x

$$[(\alpha+\beta+\gamma)F_n p_n - \alpha D_n k_n] \cosh\left(p_n \frac{b}{2}\right) - (\beta+\gamma)\frac{4(-1)^n}{ak_n} = 0$$

thus

$$F_n = \frac{\alpha}{\alpha+\beta+\gamma}\frac{D_n k_n}{p_n} + \frac{\beta+\gamma}{\alpha+\beta+\gamma}\frac{4(-1)^n}{ak_n p_n \cosh\left(p_n \frac{b}{2}\right)}$$

or

$$F_n = (1-\psi)\frac{D_n k_n}{p_n} + \psi \frac{4(-1)^n}{ak_n p_n \cosh\left(p_n \frac{b}{2}\right)} \tag{24}$$

where ψ is the polar ratio[3], $\psi = (\beta+\gamma)/(\alpha+\beta+\gamma)$.

$$t_{xx}\big|_{x=a/2} \quad \text{and} \quad t_{yy}\big|_{y=b/2}$$

are automatically satisfied, since these components of stress vanish everywhere.

Now, we have determined all the coefficients except D_n and C so far. There are two boundary conditions which remain to be satisfied

$$m_{xy}\big|_{x=a/2} = -(\beta+\gamma)\sum_{n=0}^{\infty}\frac{(-1)^n}{2}B_n k_n^2 \sinh(k_n y) - C\sum_{n=0}^{\infty}(-1)^n(\gamma F_n k_n + \beta D_n p_n)\sinh(p_n y) = 0 \tag{25a}$$

$$m_{yx}\big|_{y=b/2} = -\sum_{n=0}^{\infty}\left\{(\beta+\gamma)\frac{1}{2}B_n k_n^2 \sinh\left(k_n \frac{b}{2}\right) + C(\gamma D_n p_n + \beta F_n k_n)\sinh\left(p_n \frac{b}{2}\right)\right\}\sin(k_n x) = 0. \tag{25b}$$

At this point, reconsider field {I} alone in which the terms containing C are absent which is a special case of the above {I} + C{II}. Field {I} may be considered to be an exact analytical solution of a torsion-like problem in which couple stresses, eqns (25a) and (25b), are applied to the lateral surfaces. Solutions of this type (see also Ref. [13]) are not particularly useful to the experimentalist owing to the difficulty of applying such a specified distribution of couple stresses. Nevertheless, observe that the only way the classical warp can occur in a Cosserat prism is for such a distribution to be applied. In the absence of such tractions, the warp, hence the strain distribution must differ from the classical case, as indicated in Section 3. In the classical limit $\beta \to 0$, $\gamma \to 0$, the distributions, eqns (25a) and (25b), vanish, as expected.

In eqn (25b), by requiring each term in curly brackets to vanish, we obtain

$$(\beta + \gamma)\frac{B_n k_n^2}{2}\sinh\left(k_n\frac{b}{2}\right) + C(\gamma D_n p_n + \beta F_n k_n)\sinh\left(p_n\frac{b}{2}\right) = 0. \tag{26}$$

Upon substituting eqn (24) into eqn (26) we obtain

$$\frac{l_t^2}{2l_b^2}\frac{B_n k_n^2}{2}\sinh\left(k_n\frac{b}{2}\right) + CD_n\left[p_n + \left(\frac{l_t^2}{2l_b^2} - 1\right)(1-\psi)\frac{k_n^2}{p_n}\right]\sinh\left(p_n\frac{b}{2}\right)$$
$$+ \psi\left(\frac{l_t^2}{2l_b^2} - 1\right)\frac{4(-1)^n C}{ap_n}\tanh\left(p_n\frac{b}{2}\right) = 0 \tag{27}$$

where l_t is the torsional characteristic length[3], $l_t^2 = (\beta + \gamma)/(2\mu + \kappa)$. Substituting B_n and solving for D_n, we obtain

$$D_n = \frac{\dfrac{l_t^2}{l_b^2}\dfrac{2(-1)^n}{ak_n}\tanh\left(k_n\dfrac{b}{2}\right) + \left(\dfrac{l_t^2}{2l_b^2} - 1\right)\psi\dfrac{4(-1)^n C}{ap_n}\tanh\left(p_n\dfrac{b}{2}\right)}{C\left[p_n + \left(\dfrac{l_t^2}{2l_b^2} - 1\right)(1-\psi)\dfrac{k_n^2}{p_n}\right]\sinh\left(p_n\dfrac{b}{2}\right)}. \tag{28}$$

Now boundary condition (25b) is satisfied, condition (25a) remains to be satisfied, and the constant C remains to be determined. Since the two summations in eqn (25a) represent functions which differ in their y dependence, choice of C is insufficient to make m_{xy} vanish everywhere on the lateral boundary, although m_{xy} can be made small by a proper choice of C. Field $\{I\} + C\{II\}$ is used as follows in a superposition approach.

This approach is based on a restriction of the rectangular cross-section to be square, so that the problem is now symmetrical under 90° rotations. For a square cross-section, a field of displacement and microrotation is an equally valid solution following a 90° rotation. Figure 3 summarizes the superposition of such rotated fields to generate the field $\{I\} + C\{II\} + C\{II_{ROT}\}$ in which $\{II_{ROT}\}$ refers to field $\{II\}$ (eqns (15)) rotated by 90°.

The expanded form of the proposed solution, field $\{I\} + C\{II\} + C\{II_{ROT}\}$, in Cartesian coordinates is

$$u_x = -\theta(1 + 2C)yz \tag{29a}$$

$$u_y = \theta(1 + 2C)xz \tag{29b}$$

$$u_z = \theta xy - \theta\sum_{n=0}^{\infty} B_n \sinh(k_n y)\sin(k_n x) - \theta C\sum_{n=0}^{\infty} A_n \sinh(p_n y)\sin(k_n x)$$
$$+ \theta C\sum_{n=0}^{\infty} A_n \sin(k_n y)\sinh(p_n x) \tag{29c}$$

$$\phi_x = -\theta Cx - \theta\sum_{n=0}^{\infty} \tfrac{1}{2}B_n k_n \cosh(k_n y)\sin(k_n x) - \theta C\sum_{n=1}^{\infty} D_n \cosh(p_n y)\sin(k_n x)$$
$$+ \theta C\sum_{n=0}^{\infty} F_n \cos(k_n y)\sinh(p_n x) \tag{29d}$$

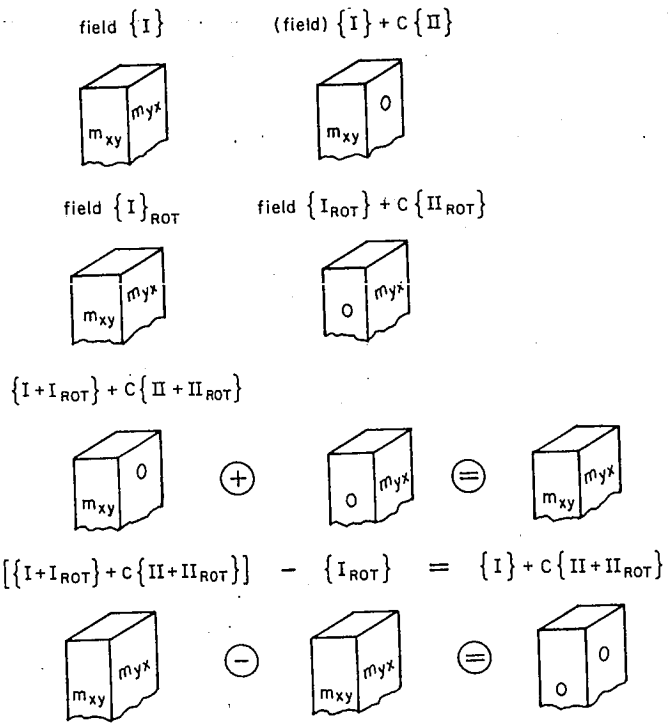

Fig. 3. Superposition of displacement–microrotation fields.

$$\phi_y = -\theta(1 + C)y + \theta \sum_{n=0}^{\infty} \tfrac{1}{2} B_n k_n \sinh(k_n y)\cos(k_n x) + \theta C \sum_{n=0}^{\infty} F_n \sinh(p_n y)\cos(k_n x) - \theta C \sum_{n=0}^{\infty} D_n \sin(k_n y)\cosh(p_n x) \tag{29e}$$

$$\phi_z = \theta(1 + 2C)z \tag{29f}$$

in which the angle of twist per unit length is now

$$\theta' = \theta(1 + 2C). \tag{30}$$

5.2. *Approximate solution*

One coefficient C remains to be determined. The value of C is determined on the basis of the following considerations. First, the displacement and microrotation field (29) must converge to the classical solution as $\gamma \to 0$ or $\kappa \to 0$. Second, the residual couple stress tractions on the lateral surface must be minimized. For field (29) these tractions are

$$m_{xy}|_{x=a/2} = 4\theta(\beta + \gamma)\Bigg\{ - \sum_{n=0}^{\infty} \sinh(k_n y)/ak_n \cosh(k_n a/2) + \sum_{n=0}^{\infty} (-1)^n \tanh(k_n a/2)\sin(k_n y)/ak_n - \sum_{n=0}^{\infty} \psi\gamma C \sinh(p_n y)/ap_n \cosh(p_n a/2) + \sum_{n=0}^{\infty} [\tanh(k_n a/2)/ak_n + \psi\beta C \tanh(p_n a/2)/ap_n] \times [\beta p_n^2 + \gamma(1 - \psi)k_n^2] \sinh(p_n y)/\sinh(p_n a/2)[\gamma p_n^2 + \beta(1 - \psi)k_n^2] \Bigg\} \tag{31}$$

$$m_{yx}|_{y=a/2} = 4\theta(\beta+\gamma)\Big\{-\sum_{n=0}^{\infty}\psi\gamma C\sinh(p_n y)/ap_n\cosh(p_n a/2) + \sum_{n=0}^{\infty}[\tanh(k_n a/2)/ak_n + \psi\beta C\tanh(p_n a/2)/ap_n] \times [\beta p_n^2 + \gamma(1-\psi)k_n^2]\sinh(p_n y)/[\gamma p_n^2 + \beta(1-\psi)k_n^2]\sinh(p_n a/2)\Big\}. \tag{32}$$

Field (29), with an appropriate choice of C, represents a very good approximation to the solution of the problem of torsion of a square Cosserat prism, with zero traction upon the lateral surfaces. Details concerning the choice of C and error analysis are given in the Appendix.

5.3. *Exact solution*

An exact solution may be constructed by a superposition of fields $\{\mathrm{I}\} + \sum_{q=1}^{\infty} C^q\{\mathrm{II}^q\}$ in which the coefficients C_n^q in each constituent field $\{\mathrm{II}\}$ are chosen so that the residual tractions m_{xy}, m_{yx} on the lateral surface are reduced as q increases. The approximation in Section 5.2 is, however, sufficiently accurate that we shall not pursue this further at present.

5.4. *Determination of torsional rigidity*

The torsional rigidity J is defined in terms of the applied twisting moment M_t; $J = M_t z/\theta'$. The twisting moment is obtained from an integration of surface tractions upon the end

$$\int_A (xt_{zy} - yt_{xz} + m_{zz})\,\mathrm{d}A = M_t. \tag{33}$$

By substituting eqns (9b), (9c), (10a), (10b) and (29a)–(29f) into eqn (33) and integrating, we obtain

$$\theta(2\mu+\kappa)\Big\{(1+2C)\frac{a^4}{12} - \sum_{n=0}^{\infty}\frac{32}{ak_n^5}\tanh\Big(k_n\frac{a}{2}\Big) + \sum_{n=0}^{\infty}\frac{8}{k_n^4} + (1+2C)l_t^2a^2 + C\Big[\sum_{n=0}^{\infty}\frac{2(-1)^n aA_n}{p_n}\cosh\Big(p_n\frac{a}{2}\Big) - \sum_{n=0}^{\infty}4(-1)^n A_n\Big(\frac{1}{k_n^2}+\frac{1}{p_n^2}\Big)\sinh\Big(p_n\frac{a}{2}\Big) + \Big(\frac{1}{\psi}-1\Big)l_t^2\sum_{n=0}^{\infty}(F_n p_n - D_n k_n)\frac{8(-1)^n}{k_n p_n}\sinh\Big(p_n\frac{a}{2}\Big)\Big]\Big\} = M_t$$

thus

$$\theta = M_t\Big/(2\mu+\kappa)\Big\{(1+2C)\frac{a^4}{12} - \sum_{n=0}^{\infty}\frac{32}{ak_n^5}\tanh\Big(k_n\frac{a}{2}\Big) + (1+2C)l_t^2a^2 + C\Big[\sum_{n=0}^{\infty}\frac{2(-1)^n aA_n}{p_n}\cosh\Big(p_n\frac{a}{2}\Big) - \sum_{n=0}^{\infty}4(-1)^n A_n\Big(\frac{1}{k_n^2}+\frac{1}{p_n^2}\Big)\sinh\Big(p_n\frac{a}{2}\Big) + \Big(\frac{1}{\psi}-1\Big)l_t^2\sum_{n=0}^{\infty}(F_n p_n - D_n k_n)\frac{8(-1)^n}{k_n p_n}\sinh\Big(p_n\frac{a}{2}\Big)\Big]\Big\}. \tag{34}$$

We obtain for the rigidity

$$J' = G\left\{\frac{(1+C)a^4}{(1+2C)3} - \frac{64}{(1+2C)}\sum_{n=0}^{\infty}\frac{1}{ak_n^5}\tanh\left(k_n\frac{a}{2}\right) + 2l_t^2a^2\right.$$
$$+\frac{C}{1+2C}\left[\sum_{n=0}^{\infty}\frac{4(-1)^n aA_n}{p_n}\cosh\left(p_n\frac{a}{2}\right) - \sum_{n=0}^{\infty}8(-1)^nA_n\left(\frac{1}{k_n^2}+\frac{1}{p_n^2}\right)\sinh\left(p_n\frac{a}{2}\right)\right.$$
$$\left.\left.+\left(\frac{1}{\psi}-1\right)l_t^2\sum_{n=0}^{\infty}(F_np_n - D_nk_n)\frac{16(-1)^n}{k_np_n}\sinh\left(p_n\frac{a}{2}\right)\right]\right\} \tag{35}$$

in which we have incorporated

$$\sum_{n=0}^{\infty}\frac{1}{(2n+1)^4} = \frac{\pi^4}{96}$$

and the micropolar shear modulus G is given by $(2\mu + \kappa) = 2G$. The torsional rigidity for classical elasticity theory is[9]

$$J = G\left\{\frac{a^4}{3} - 64\sum_{n=0}^{\infty}\frac{1}{ak_n^5}\tan\left(k_n\frac{a}{2}\right)\right\}. \tag{36}$$

One common feature of solutions of boundary-value problems in micropolar elasticity theory is that they predict a stiffening effect which depends on the size of a specimen of material. This stiffening effect is predicted in the bending of plates[3] as well as beams[14] and in the torsion of rods[3]. The predicted stiffening is manifested in part in the term containing a^2 in eqn (35). Such terms also appear in the simpler exact analytical solutions for Cosserat solids presented in Refs [3, 14]. The stiffening effect becomes noticeable if the specimen cross-section is ten times the characteristic length, and can become large as the specimen cross-section approaches the characteristic length. Neither stiffening nor size effects are predicted in tension.

Eringen[8] uses the principle of non-negative internal energy to impose certain restrictions on the micropolar elastic moduli. They are

$$\begin{aligned} &0 \leqslant 3\lambda + 2\mu + \kappa, \quad && 0 \leqslant 2\mu + \kappa, \quad && 0 \leqslant \kappa \\ &0 \leqslant 3\alpha + \beta + \gamma, \quad && -\gamma \leqslant \beta \leqslant \gamma, \quad && 0 \leqslant \gamma. \end{aligned} \tag{37}$$

After some manipulation, one obtains the corresponding range of the material parameters: $0 \leqslant N \leqslant 1$, $l_t \geqslant 0$, $l_b \geqslant 0$, $0 \leqslant \psi \leqslant 3/2$, $-1 \leqslant \beta/\gamma \leqslant 1$, $-1 \leqslant \nu' \leqslant 0.5$, where ν' is Poisson's ratio of micropolar elasticity[14], $\nu' = \lambda/(2\lambda + 2\mu + \kappa)$.

Denoting the ratio of micropolar to classically elastic torsional rigidity, J'/J by Ω in eqns (35) and (36) it is observed that Ω increases with N. When N becomes zero, the classical result $\Omega = 1$ is obtained. Also, Ω increases with l_t and as l_t becomes zero, Ω becomes unity. Therefore, we obtain the classical result in the limit, as required by the fact that classical elasticity is a special case of micropolar elasticity. Figures 4–7 are graphical representations of the torsional rigidity. Figures 4 and 5 display the influence of the material constants upon the torsional rigidity ratio, Ω. Figure 6 shows the influence of N upon the rigidity in J'/a^2–a^2 curves with $\psi = 1.5$, $l_t = 0.2$ mm and $\beta/\gamma = 0.5$. Figure 7 shows the influence of l_t upon the rigidity in J'/a^2–a^2 curves with $\psi = 1.5$, $\beta/\gamma = 0.5$ and $N = 0.9$. These results are similar to those obtained by other authors[3, 14] in other geometries in that a stiffening effect is predicted. They are similar to those for torsion of a cylindrical bar[3] in that stiffening effects are most noticeable for large l_t and large N, and that ψ has little effect when $l_t \ll a$. The present results differ from Ref. [3] in that for

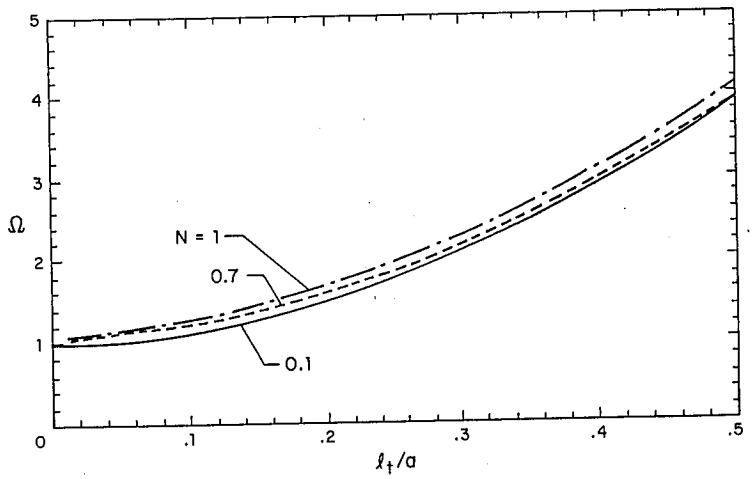

Fig. 4. Rigidity ratio Ω vs characteristic length: dependence on N for $\psi = 1.5$, $\beta/\gamma = 0.5$.

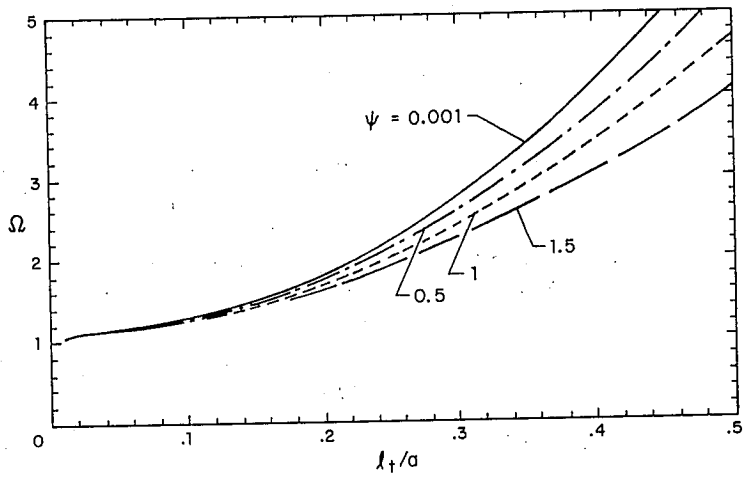

Fig. 5. Rigidity ratio Ω vs characteristic length: dependence on ψ for $N = 0.9$, $\beta/\gamma = 0.5$.

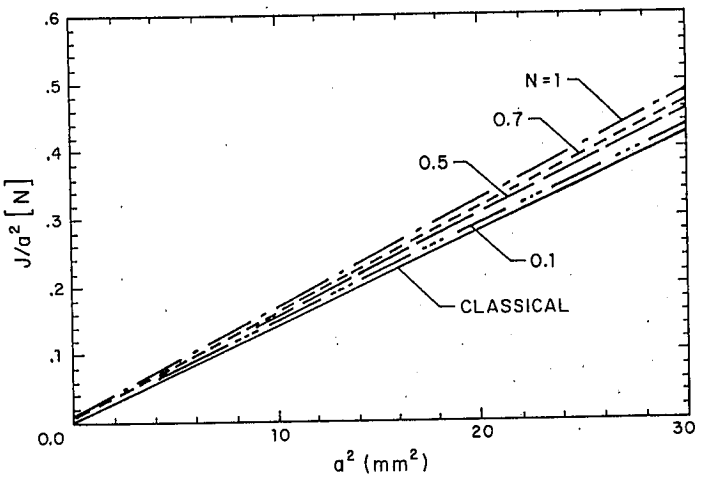

Fig. 6. Rigidity divided by diameter squared vs diameter squared, dependence on N, for $l_t = 0.2$ mm, $\psi = 1.5$, $\beta/\gamma = 0.5$.

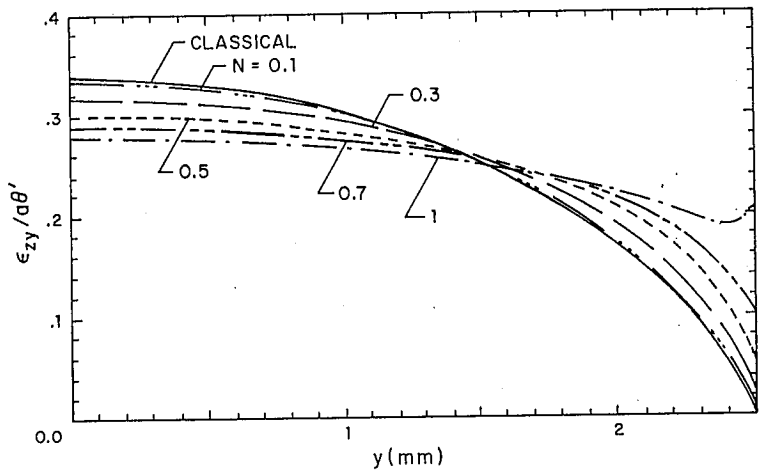

Fig. 8. Normalized shear strain along lateral surface $x = a/2$ vs position: dependence on N for $\psi = 1.5$, $\beta/\gamma = 0.5$, $l_t = 0.2$ mm.

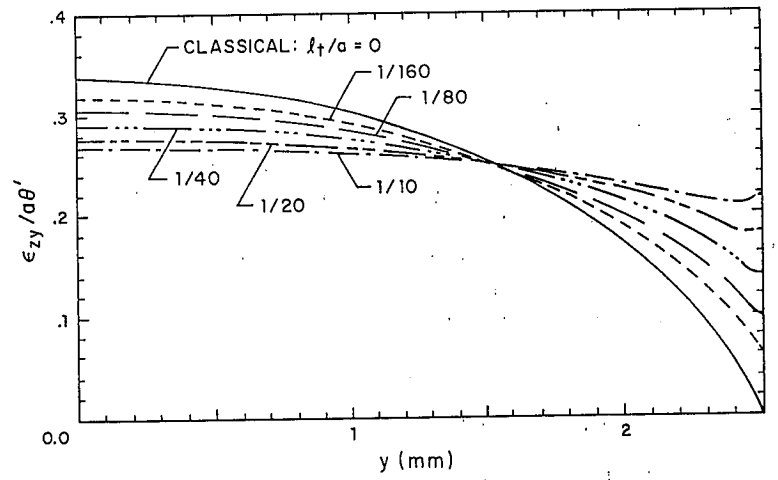

Fig. 9. Normalized shear strain along lateral surface $x = a/2$ vs position: dependence on characteristic length divided by bar width, for $\psi = 1.5$, $\beta/\gamma = 0.5$.

on the boundary. Strains are normalized by dividing by the twist angle and width of the cross-section. As anticipated in Section 3, a non-zero shear strain is predicted to occur at the corners of the cross-section when the bar is made of a micropolar material. Numerical tests described in the Appendix were performed to test the validity of the approximate solution in predicting a non-zero corner stress. On the basis of these tests it is concluded that the predicted non-zero stress and strain are valid and are not an artifact of the approximation scheme.

7. EXPERIMENTAL MODALITIES

The analysis presented in this article makes possible the design of new kinds of experiments for the study of Cosserat elastic solids. Some of these experimental modalities confer significant advantages over existing ones.

7.1. *Size effects*

The first approach to be considered is a method of size effects based on the torsional rigidity of square bars obtained in Section 5.4. As in the case of rods of circular cross-section[3], predicted rigidity of slender bars of a Cosserat solid exceeds the rigidity of a corresponding classical solid of the same shear modulus. Size effect studies in square bars

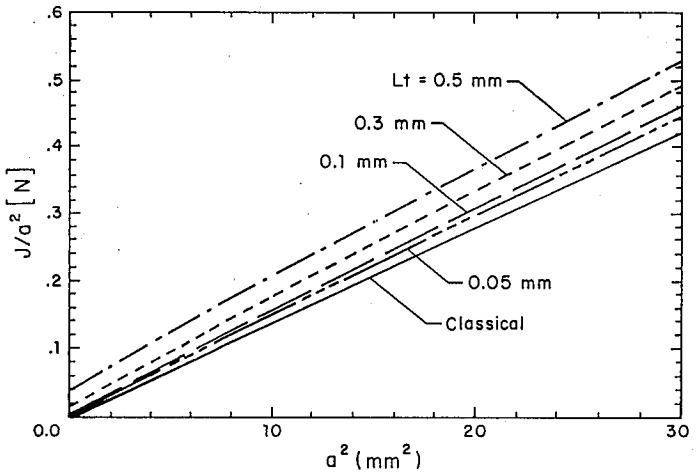

Fig. 7. Rigidity divided by diameter squared vs diameter squared, dependence on l_t for $N = 0.9$, $\psi = 1.5$, $\beta/\gamma = 0.5$.

small specimens approaching l_t in thickness, stiffening effects can become large even for small N, regardless of the value of ψ, whereas in Ref. [3] stiffening effects become large only for $N \cong 1$ or for ψ very different from 1.5. For larger specimens of thickness about 16 times the torsional characteristic length, the square cross-section prism is stiffened by about 20% while the circular cylindrical rod[3] is stiffened by about 10%. This difference can be attributed to the fact that strain gradients are greater in the square cross-section case. These differences in the solutions for different geometries may be useful in the determination and consistency tests of the micropolar elastic constants.

6. STRAIN DISTRIBUTION ACROSS THE LATERAL SURFACE

The tensorial shear strain, $e_{zy} = \frac{1}{2}(u_{z,y} + u_{y,z})$, obtained from the displacement field (29), upon the boundary $x = a/2$, is as follows:

$$e_{zy}|_{x=a/2} = \frac{\theta}{2}\left\{2(1+C)a - \sum_{n=0}^{\infty} \frac{8}{ak_n^2 \cosh\left(k_n \frac{a}{2}\right)} \cosh(k_n y) - \sum_{n=0}^{\infty} CA_n p_n (-1)^n \cosh(p_n y) + \sum_{n=0}^{\infty} CA_n k_n \sinh\left(p_n \frac{a}{2}\right) \cos(k_n y)\right\} \tag{38}$$

where $k_n = (2n+1)\pi/a$, $p_n = [k_n^2 + (N/l_b)^2]^{1/2}$ and

$$A_n = \frac{8(-1)^n(1-N^2)}{ak_n^2 p_n \cosh\left(p_n \frac{a}{2}\right)} - \frac{\frac{l_t^2}{l_b^2}\frac{4(-1)^n N^2}{k_n}\tanh\left(k_n \frac{a}{2}\right) + \left(\frac{l_t^2}{2l_b^2} - 1\right)\frac{8(-1)^n \psi C}{p_n}\tanh\left(p_n \frac{a}{2}\right)}{Ca\left[p_n^2 + \left(\frac{l_t^2}{2l_b^2} - 1\right)(1-\psi)k_n^2\right]\sinh\left(p_n \frac{a}{2}\right)}.$$

Figures 8 and 9 show the influence of material parameters upon the shear strain distribution

may be used (i) in comparison with results obtained with circular cross-sections as an internal consistency test of the Cosserat model of a material, and (ii) as a primary method to be used for materials which cannot be easily formed in a circular cylindrical form, but which can be readily cut; for example, a flexible polymer foam.

7.2. *Strain distribution; strain at the corner*

As shown in Section 6, the strain distribution across the lateral surface of a Cosserat prism differs from that in a classically elastic prism. By measuring this strain distribution via strain gages or by optical methods, one should be able to distinguish between classical and Cosserat elastic materials. Since measurements upon a single specimen suffice to demonstrate the presence of non-classical effects, this approach is simpler than the method of size effects which requires an ensemble of progressively smaller specimens to be machined. In addition, a method based on measurement of the strain distribution permits the use of specimens very much larger than the microstructure size.

The reason for this is that a finite Cosserat characteristic length always results in a non-zero shear strain along the edges of the twisted bar, while a classical bar exhibits zero strain along the edges. If the characteristic length is small compared to the bar width, the non-classical strain at the edge is small compared to the strain at the center of the lateral surface, but it differs from zero. The percent difference between a zero strain and a non-zero strain is infinite, whereas in the method of size effects the percent difference between the rigidity of two bars or rods of different sizes much larger than the characteristic length, is small. Now practical strain-measurement techniques always have a finite gage length and a limit to resolution, so it is not possible to measure arbitrarily small strain exactly at the edge. Nevertheless, this method should permit the evaluation of Cosserat elastic behavior in specimens much larger than the characteristic length.

7.3. *Stress at the corner*

The presence of non-classical shear stress at the corner of the cross-section may be inferred by making a small nick or crack in the corner of a twisted bar. The crack will open in mode III if the bar is made of a Cosserat solid, since non-zero stresses are relieved. By contrast a similar crack in a classically elastic bar shows no tendency to open. Experiments have been conducted on the basis of this approach, using holographic methods[15], and in the context of lecture demonstration experiments[16]. It was found that a small corner crack in a twisted bar of rubber[16] or of polymethyl methacrylate[15] did not open, as expected from the classical prediction and the known classical behavior of such homogeneous materials. By contrast, a similar corner crack in a twisted bar of low density polymer foam[16] or of high density foam[15] was observed to open. Such a phenomenon is consistent with the predictions presented in this article and with evidence based on size-effect studies that these structured materials behave as Cosserat solids[7, 17].

8. CONCLUSION

The problem of torsion of a Cosserat elastic bar of square cross-section has been solved. Size effects in the torsional rigidity are predicted to occur. Stress and strain are predicted to be nonzero at the corners of the cross-section, in contrast to the classical case. Experimental methods based on these predictions offer a variety of advantages over currently available methods.

REFERENCES

1. J. Schijve, *J. Mech. Phys. Solids* **14,** 113 (1966).
2. R. W. Ellis and C. W. Smith, *Expl Mech.* **7,** 372 (1968).
3. R. D. Gauthier and W. E. Jahsman, *J. Appl. Mech.* **42,** 369 (1975).
4. J. F. C. Yang and R. S. Lakes, *J. Biomech. Engng* **103,** 275 (1981).
5. R. S. Lakes, *J. Biomech. Engng* **104,** 6 (1982).
6. J. F. C. Yang and R. S. Lakes, *J. Biomechanics* **15,** 91 (1982).

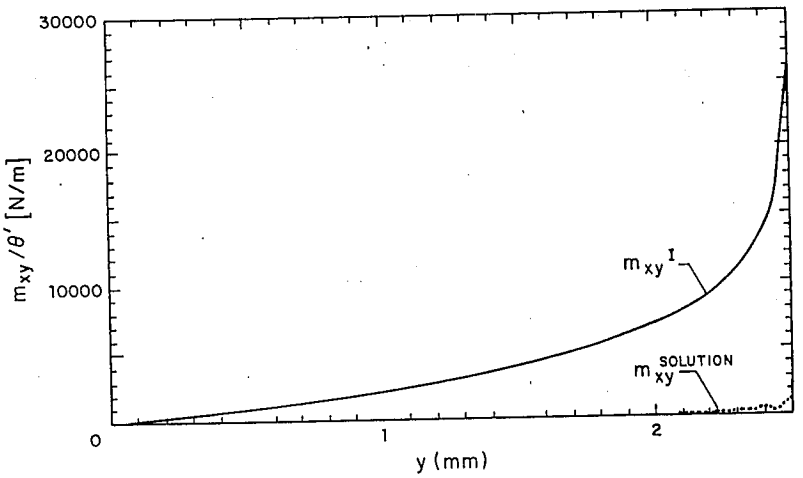

Fig. 10. Violation of the boundary condition $m_{xy} = 0$ for field I and for the approximate solution, vs position. $N = 0.9$; $l_t/a = 0.04$, $\psi = 1.5$ and $\beta/\gamma = 0.5$.

7. R. S. Lakes, *Int. J. Solids Structures*, **22**, 55 (1986).
8. A. C. Eringen, *Fracture* (Edited by M. Liebowitz), Vol. 2, pp. 621–729. Academic Press, New York (1968).
9. I. S. Sokolnikoff, *Mathematical Theory of Elasticity*, 2nd edn. McGraw-Hill, New York (1956).
10. D. Iesan, *Int. J. Engng Sci.* **9**, 879 (1971).
11. D. Iesan, *Int. J. Engng Sci.* **9**, 1047 (1971).
12. S. C. Cowin, *J. Appl. Math. Phys. (ZAMP)* **21**, 494 (1970).
13. A. C. Smith, *Int. J. Engng Sci.* **5**, 637 (1967).
14. G. V. Krishna Reddy and N. K. Venkatasubramanian, *J. Appl. Mech.* **45**, 429 (1978).
15. R. S. Lakes, W. Bonfield and D. Gorman, *J. Materials Sci.* **20**, 2882 (1985).
16. R. S. Lakes, *Mech. Monograph* **M5**, 1 (1985).
17. R. S. Lakes, *J. Materials Sci.* **18**, 2572 (1983).
18. H. C. Park, Ph.D. dissertation. Department of Mechanical Engineering, University of Iowa (1985).

APPENDIX: ERROR ESTIMATES

The displacement-microrotation field in eqns (29a)–(29f) represents the solution to a torsion problem in which couple stresses given by eqns (31) and (32) are applied to the lateral surfaces. These couple stresses depend upon the choice of the coefficient C; they can be minimized by the proper choice of C. The field in eqns (29a)–(29f) then becomes an approximate solution to the standard torsion problem in which zero traction is applied to the lateral surfaces.

C is determined by: (i) requiring the surface tractions, eqns (31) and (32) to be minimized in a root-mean-square sense and (ii) requiring the proposed solution, eqns (29a)–(29f) to approach the classical solution when κ or γ approach zero in the classical limit. To achieve (i), define error measures ξ and η:

$$\xi = \left[\int_0^{a/2} (m_{xy}^{\mathrm{I+CII+CII_{ROT}}}|_{x=a/2})^2\,\mathrm{d}y \Big/ \int_0^{a/2} (m_{xy}^{\mathrm{I}}|_{x=a/2})^2\,\mathrm{d}y\right]^{1/2} \tag{A1}$$

$$\eta = \left[\int_0^{a/2} (m_{yx}^{\mathrm{I+CII+CII_{ROT}}}|_{y=a/2})^2\,\mathrm{d}x \Big/ \int_0^{a/2} (m_{yx}^{\mathrm{I}}|_{y=a/2})^2\,\mathrm{d}x\right]^{1/2}. \tag{A2}$$

The rationale is that the unwanted couple stress traction on the lateral surface (violation) in field $\{\mathrm{I}\}$ is sufficient to maintain the warp, hence the surface strain, identical to that of a classical bar. The quantity ξ can be considered as an estimate of the error in the deviation of the warp from classical values, in field $\{\mathrm{I}\} + C\{\mathrm{II}\} + C\{\mathrm{II_{ROT}}\}$.

As a test of numerical procedures, the quantities ξ and η are calculated in two ways: by explicitly carrying out the operations in eqns (A1) and (A2) termwise[18], and by numerically integrating as follows:

$$\xi = \left\{\left[\sum_{i=1}^{q} (m_{xy}^{\mathrm{I+CII+CII_{ROT}}}(y_i)|_{x=a/2})^2\right] \Big/ \left[\sum_{i=1}^{q} (m_{xy}^{\mathrm{I}}(y_i)|_{x=a/2})^2\right]\right\}^{1/2}. \tag{A3}$$

A further test of the numerical procedures is to compare ξ and η which must be equal in view of the rotational symmetry of a square bar.

Results of the analysis are as follows. For a material for which $N = 0.9$, $\psi = 1.5$, $l_t/a = 0.04$, $\beta/\gamma = 0.5$ ($l_t/l_b = [2(1 + (\beta/\gamma))]^{1/2} = \sqrt{3}$), the error measures based on a numerical integral [eqn (A3)] are $\xi = 0.019$ and $\eta = 0.022$, for the optimal value of C. The corresponding quantities obtained by termwise integration [eqns (A1), (A2)] are $\xi = 0.023$ and $\eta = 0.023$. A plot of the residual violation of $m_{xy} = 0$ on the boundary is shown in Fig. 10.

An alternative error measure was also tried:

$$\xi_1 = \left\{\frac{1}{q}\sum_{i=1}^{q}\left[m_{xy}^{I+CII+CII_{ROT}}(y_i)/m_{xy}^{I}(y_i)\big|_{x=a/2}\right]^2\right\}^{1/2}. \tag{A4}$$

This resulted in smaller values of the error estimate for the above hypothetical material: $\xi = 0.016$ and $\eta = 0.017$, and much smaller values than eqns (A1)–(A3) under conditions of large error. Error measures defined by (A1) and (A2) were used to obtain values of C used to generate the graphs.

The optimum value of C which minimizes the error depends on the elastic constants in a complex way. Nevertheless, a choice of C given by $C = 25Nl_t/a$ is sufficient to ensure that $\xi \leqslant 0.10$ over a wide range of N, l_t and ψ, and for $0 \leqslant \beta/\gamma \leqslant 0.6$.

Further numerical studies were performed to explore the effects of the error terms on the strain distribution. In these studies, the quantity C was perturbed from its optimal value. It was observed that the boundary condition violation m_{xy} could be made positive or negative over the entire lateral surface. The predicted strain distribution, however, varied only slightly. Furthermore, the perturbation of C was in no case observed to cause the corner strain to vanish or to change sign in a micropolar material. It is concluded that ξ and η are reasonable error measures, that the error in the approximate solution is small, and that the prediction of non-zero corner strain is valid.